Optimal piston crevice study in a rapid compression machine

Optimal piston crevice study in a rapid compression machine

Oku Nyong[1], **Robert Woolley**[2], **Simon Blakey**[3], **Ehsan Alborzi**[4]
[1-4] Low Carbon Combustion Centre, University of Sheffield, UK

E-mail: meq11oen@sheffield.ac.uk

Abstract. Multi-dimensional effects such as vortex generation and heat losses from the gas to the wall of the reactor chamber have been an issue to obtaining a reliable RCM data. This vortex initiates a flow in the relatively cold boundary layer, which may penetrate the core gas. This resulting non-uniformity of the core region could cause serious discrepancies and give unreliable experimental data. To achieve a homogenous temperature field, an optimised piston crevice was designed using CFD modelling (Ansys fluent). A 2-Dimensional computational moving mesh is assuming an axisymmetric symmetry. The model adopted for this calculation is the laminar flow model and the fluid used was nitrogen. To get the appropriate crevice volume suitable for the present design, an optimisation of the five different crevice volume was modelled which resulted to about 2-10% of the entire chamber volume. The use of creviced piston has shown to reduce the final compressed gas temperature and pressure in the reactor chamber. All the crevice volumes between 2-10% of the chamber volume adequately contained the roll up vortexes, but the crevice volume of 282 mm^3 was chosen to be the best in addition to minimising the end gas pressure and temperature drop. The final pressure trace from experiment shows a reasonable agreement with the CFD model at compression and post compression stage.

1. Introduction

Rapid Compression Machine (RCM) is an essential tool when investigating auto-ignition delay time and chemical kinetics of hydrocarbon fuels. It has an advantage of producing longer compression time of more than 20ms. Its accessibility to study combustion at conditions relevant to engines and gas turbines than other reactor facilities such as flow reactor, jet stirred reactor and shock tubes. Detailed combustion kinetic mechanism could be validated using an RCM experiments [1-5]. This help provides a better understanding of the ignition phenomena that is very pertinent to improving the performance efficiency and emission characteristic of engines[6].

One of the challenges confronting the use of RCM's designs is the complex fluid dynamics features exist in the reaction chamber. These feature result from the piston motion; a roll up vortex is formed creating a non-uniform temperature profile in the chamber [7-11]. The gases in the relatively cold boundary layer mix with the hot core gas resulting in a distribution of temperatures. This hinders the homogeneity of the core region where combustion kinetics is bound to exist. The mixing of cold boundary gases with the core gas in the chamber has a negative impact on experimental data since it causes thermal stratification within the charge making it difficult to interpret results and giving misleading results. To adequately study the combustion kinetic in RCM, it should be designed to minimise fluid motion effect that could lead to a discrepancy in data. And the effect of heat loss should also be taken into account to define the reaction chamber temperature through a simple model adequately. The model is based on a common assumption that there is an adiabatic core in the RCM, which means the temperature can be calculated. In this context, the 'Core Area' is referred to the region where the bulk gases exist in the reactor chamber and are not influenced by heat loss. The temperature

distribution with the combustion chamber is typically controlled with the use of a crevice on the edge of the piston, which suppresses vortex formation [9, 11, 12]. This ideal first was initiated by Park[13] and further developed by Lee and Hochgreb[14]. The improvement was made on Park's design by changing the overall geometry of the crevice as well as increasing the original cross-sectional volume of the crevice. It was also proven that their piston crevice was adequate to suppress the roll up vortex generated in their RCM. Further computational fluid dynamics work has been used to study the physic of the roll up vortex structure, formation, temperature homogeneity[8] and also have been characterised by experiment[15] and computational investigations[12, 16-19]. The design of the crevice depends on the boundary layer thickness, which itself depends on the conditions during compression [12].

In this work, CFD study has been performed to determine the right piston crevice design that would conveniently contain the roll up vortexes and maintain a homogenous environment that would be conducive for autoignition study in the present RCM. The CFD work aimed to determine a piston crevice volume that would maintain a uniform temperature profile, minimise the compressed gas pressure and temperature in the reactor chamber.

2. Computational specification

The RCM has a cylindrical combustion chamber of 40 mm bore. The combustion chamber is oriented with the piston moving horizontally and has a stroke of 142 mm. A transient 2-D computational mesh was used, axisymmetric symmetry was assumed, and the resolution increased near the walls. Modelling was performed using Ansys Fluent. The actual machine was not truly symmetrical, because of the inlet manifold, air inlet port, and pressure transducers have modified the geometry. No slip is assumed at the cylindrical wall boundary, a uniform wall temperature of 298 K was also assumed. The compression time was approximately 30.8 ms from an initial pressure of 1bar. A mesh sensitivity study was carried out using four different angles for every time step. The highest step size (δt) was 0.25 and subsequent time step was generated by dividing by a factor of 2 to get the following 0.0125, 0.0625, 0.03125 and 0.015625. It is observed that time step greater than 0.03125 resulted in negative cell volume. To limit the computational time as well as avoiding convergence problems with the use of higher time step. A value of 0.03125 was used corresponding to the time-step size of 22.57μs for both compression stroke and post compression period was reported in all the CFD simulations. The thermal properties were generated from the NIST [20] database and specified as temperature dependent polynomials. The governing equations for the model are the conservation of energy, momentum and mass. The laminar flow model was adopted as it has been shown that it can adequately describe the experimental pressure history and velocity field inside a rapid compression machine [16, 21, 22]. The segregated implicit solver with pressure-implicit split-operator (PISO) algorithm [23] was used for pressure-velocity coupling. The pressure staggering option (PRESTO) was chosen as it prevents errors from the interpolation and pressuregradient assumptions on boundaries are prevented [24].

This scheme works better for problems with high body forces (swirl) and the second order upwind discretization for density and momentum. The second order upwind scheme changes a differential equation into an algebraic equation by Taylor series. It is more preferred than the first order scheme because it is more accurate. However, is more computationally expensive. The Navier-Stokes equation is solved along with the energy and species transport equations for all species. This evaluates a set of equations dependent on the input in fluent is represented by the following equations based on the 2D modelling.

$$\frac{\partial \rho}{\partial t} + \nabla.(\rho \boldsymbol{u}) = 0 \tag{1}$$

$$\frac{\partial \boldsymbol{u}}{\partial t} + (\boldsymbol{u}.\nabla)\boldsymbol{u} = -\frac{1}{\rho}\nabla p + \frac{\mu}{\rho}\nabla^2 \boldsymbol{u} + \boldsymbol{F} \tag{2}$$

$$\rho\left(\frac{\partial E}{\partial t} + \boldsymbol{u}.\nabla E\right) - \nabla.(k_H \nabla T) + p\nabla.\boldsymbol{u} = 0 \tag{3}$$

Where u is the velocity field vector, T is the temperature, p is the pressure, E is the internal energy, ρ is the density,μ is the viscosity,K_H is the heat conduction coefficient and F is the force per unit mass. This equations 1, 2 and 3 are the continuity, momentum and, energy equation respectively. The above equation cannot be solve to give analytical result, but solved in a discretized form. The Ansys fluent operate in a fashion by developing a result using the finite volume method and integrating the above equation to give the desired result.

The velocity profile was derived from raw experimental pressure trace as employed by Mittal [25] shown in figure 1. The piston initially starts from rest and travels with a constant velocity at a point; it follows a constant speed before decelerating to rest at a constant rate. The section is divided into a three-time period of the piston motion, which is illustrated in equation 4. This equation is relevant for the numerical calculation where the parameters are used to model the compression stroke of the RCM.

$$\boldsymbol{t_{comp} = t_{accel} + t_{const} + t_{decel}} \quad (4)$$

Where $\boldsymbol{t_{comp}}$ overall compression time, $\boldsymbol{t_{accel}}$ acceleration time, $\boldsymbol{t_{const}}$ constant velocity time and $\boldsymbol{t_{decel}}$ deceleration time. This profile is used as the user define function in the CFD for describing the piston trajectory.

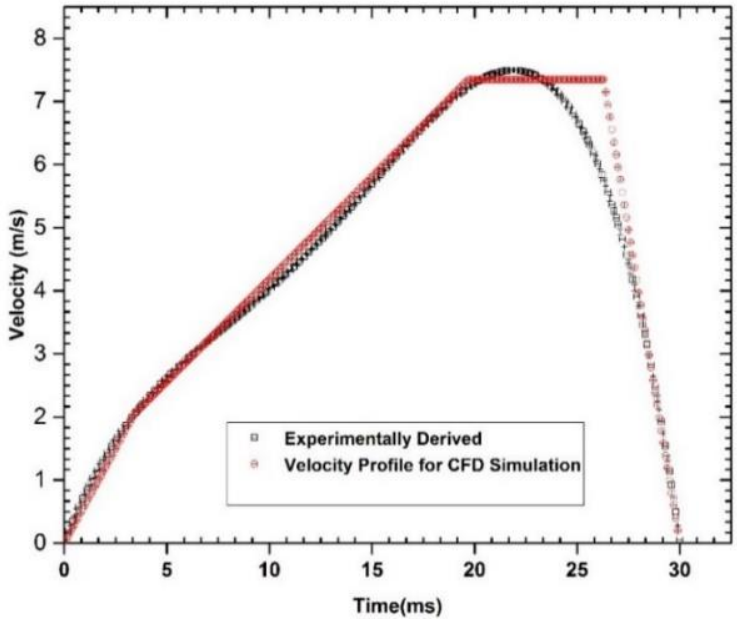

Figure 1. Piston velocity profile for 4 bar driving pressure obtained from the experimental pressure trace

.

Table 1 shows the dimensions of the piston crevice volume in mm.

Table 1. Dimensions of the piston crevice volume in mm

	Crevice Volume (mm^3)	Clearance between piston and wall	Inclined Angle. a	b	c	Height of Crevice d
1	282	0.2	15º	2.53	4	14
2	564	0.2	15º	3.58	4	14
3	846	0.2	15º	4.39	4	14
4	1128	0.2	15º	5.06	4	14
5	1143	0.2	15º	5.66	4	14

Figure 2, shows a typical computational mesh at the end of the stroke for flat and crevice piston. The mesh shown to consist of 20,042 and 26,042 cells respectively, fine grids were used on the walls and piston face and coarse meshes in between the piston and the top dead centre (TDC) to adequately capture the fluid flow taking place in the chambers. Table 1, shows five different crevice volume that was considered in this study.

(a) (b)

Figure 2. 2D computational grid for Flat and Crevice piston.

3. Results

3.1 Flat piston

Figure 3, shows the compressed gas temperature contour and velocity profile at the end of compression and up to 17 ms post compression time. The use of flat piston produces a vortex which is demonstrated in the figure below. At the post-compression stage where ignition delay is bound to occur the vortex brought to settle in the core region of the chamber and found to be severe with time distorting the homogeneity of the temperature field in the chamber.

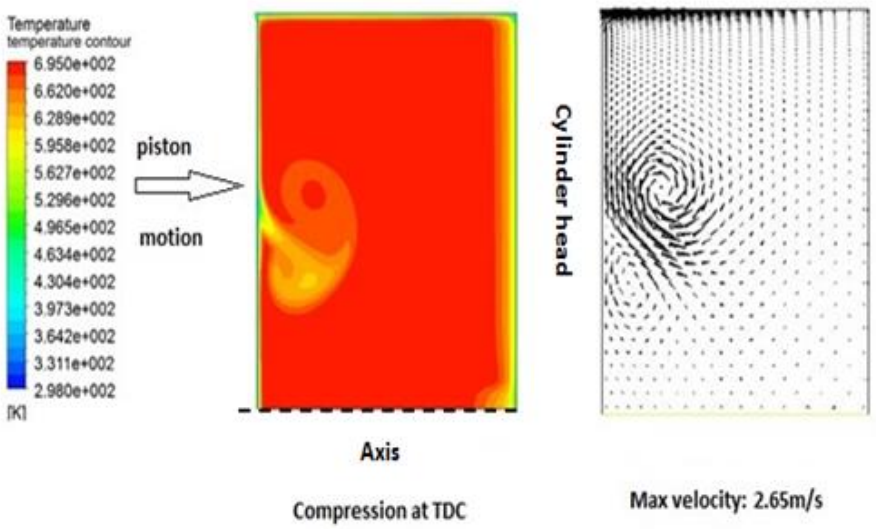
Temperature
temperature contour
6.950e+002
6.620e+002
6.289e+002
5.958e+002
5.627e+002
5.296e+002
4.965e+002
4.634e+002
4.304e+002
3.973e+002
3.642e+002
3.311e+002
2.980e+002
[K]
piston
motion
Axis
Compression at TDC
Cylinder head
Max velocity: 2.65m/s

(a)

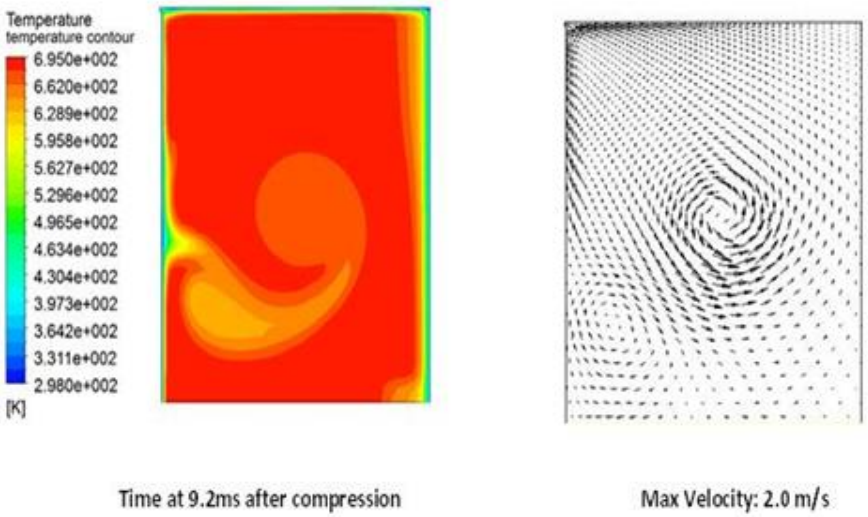
Temperature
temperature contour
6.950e+002
6.620e+002
6.289e+002
5.958e+002
5.627e+002
5.296e+002
4.965e+002
4.634e+002
4.304e+002
3.973e+002
3.642e+002
3.311e+002
2.980e+002
[K]
Time at 9.2ms after compression
Max Velocity: 2.0 m/s

(b)

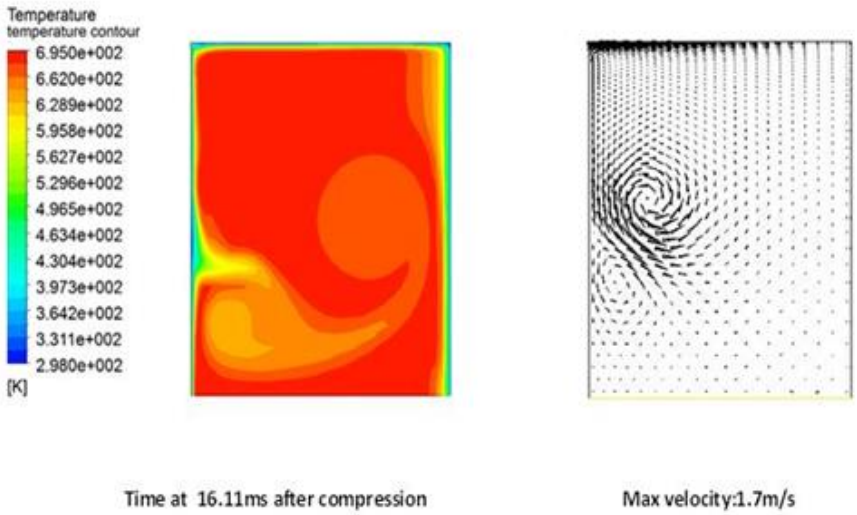

(c)

Figure 3. Contour of velocity and temperature profile for Flat piston head at Ti = 298K, Pi = 0.7 bar. (a). Compression time at TDC (b). 9.2 ms after post compression time (c). 16.11 ms after post compression time.

3.2 Crevice piston

The piston crevice with 2% of the entire chamber volume, 282mm^3, was the best at suppressing the boundary layer and providing uniform temperature field with a minimum drop in compressed gas temperature and pressure. Figure 4, presents the contour temperature profile for different crevice volume from (a-e). All the crevice volumes used contained the vortex but tends to have a reduced compressed gas temperature/pressure as the crevice volume is increased from 282 – 1410 mm^3. Figure 5, shows the isometric view of the crevice piston that was finally machined for the present RCM.

Figure 6(a), shows the final compressed gas pressure at the current condition and in comparison with the experimental pressure trace. There seems to be an agreement between the CFD model and the experiment. Matching pressure traces gives an estimated compressed gas temperature as shown in Figure 6(b).

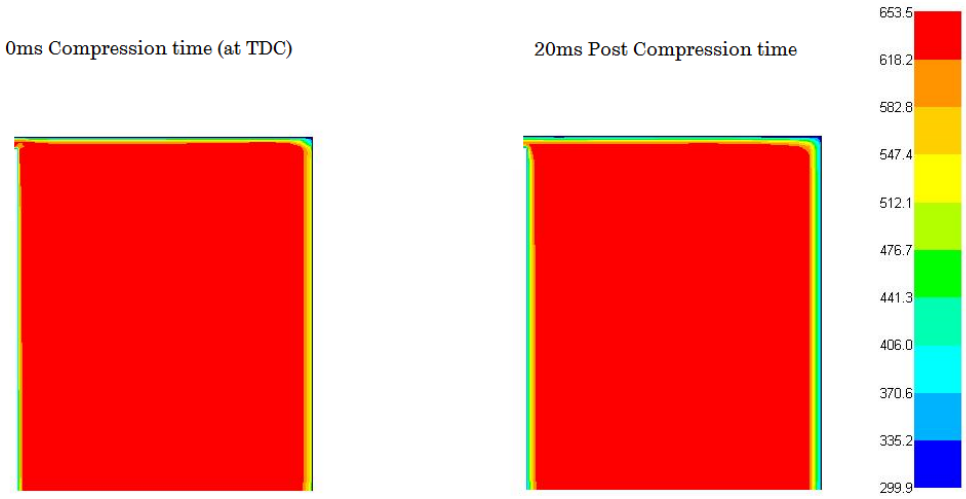

(a)

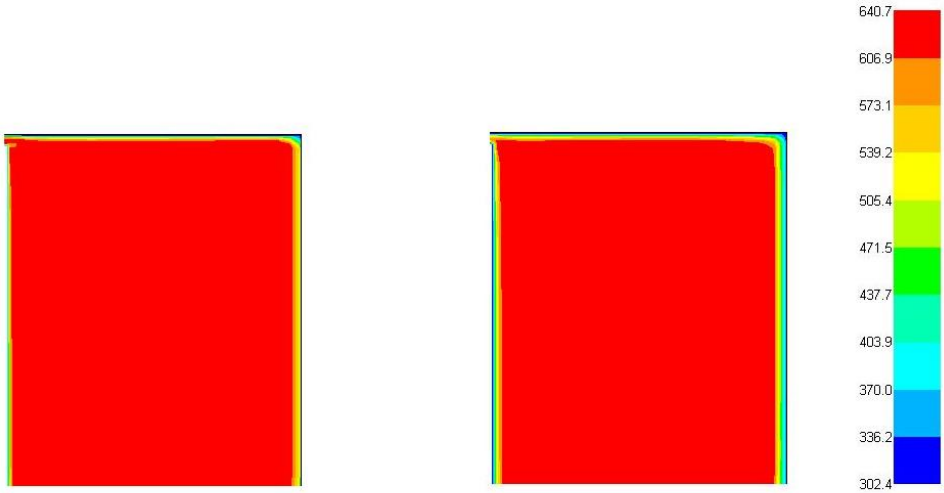
640.7
606.9
573.1
539.2
505.4
471.5
437.7
403.9
370.0
336.2
302.4

(b)

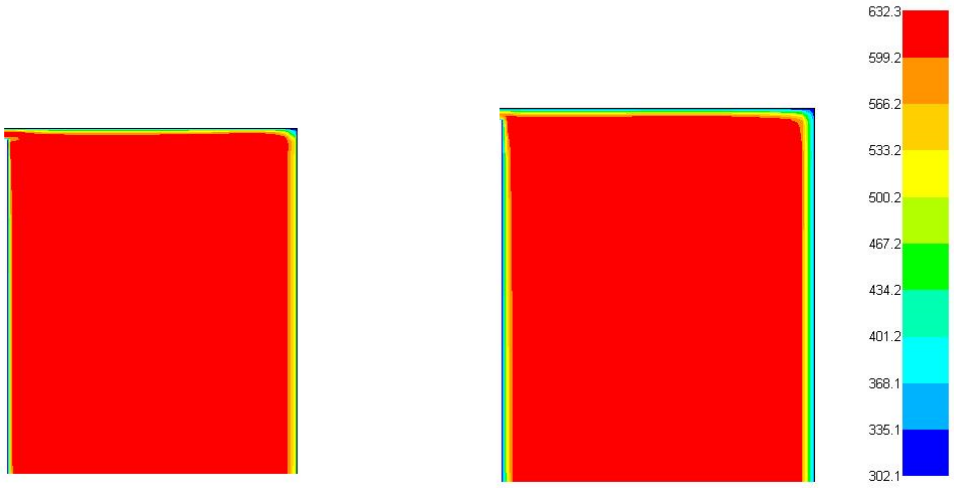
632.3
599.2
566.2
533.2
500.2
467.2
434.2
401.2
368.1
335.1
302.1

(c)

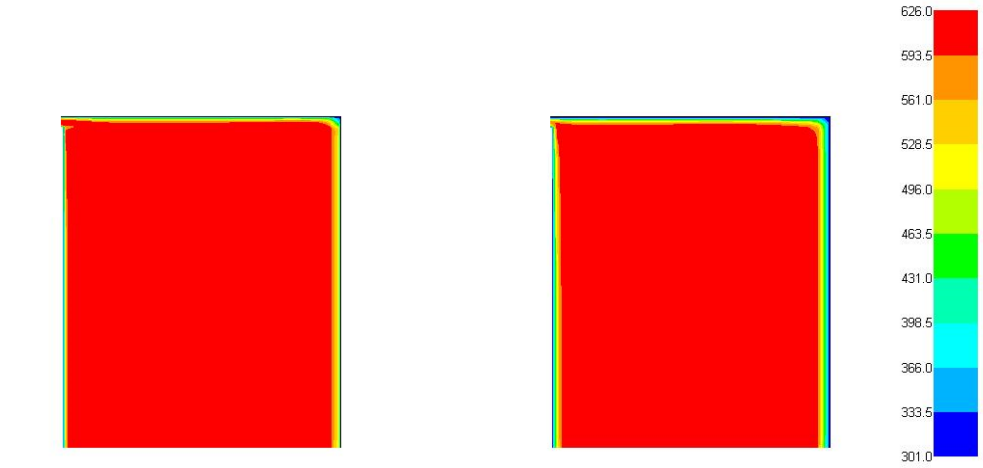

(d)

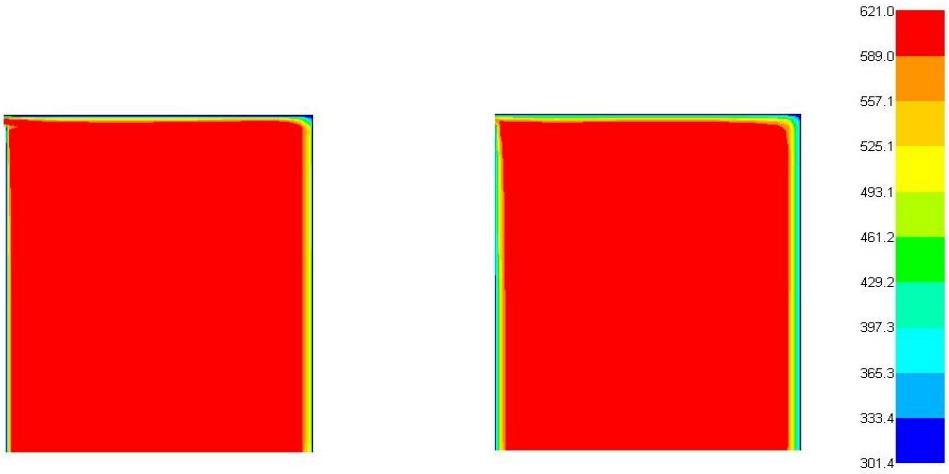

(e)

Figure 4. Shows the contour of the compressed gas temperature profile for piston crevice head with angled channel. (a) volume = 282 mm^3 (b) volume = 564 mm^3 (c) Volume = 846 mm^3 (d) Volume = 1128 mm^3 (e) volume 1410 mm^3

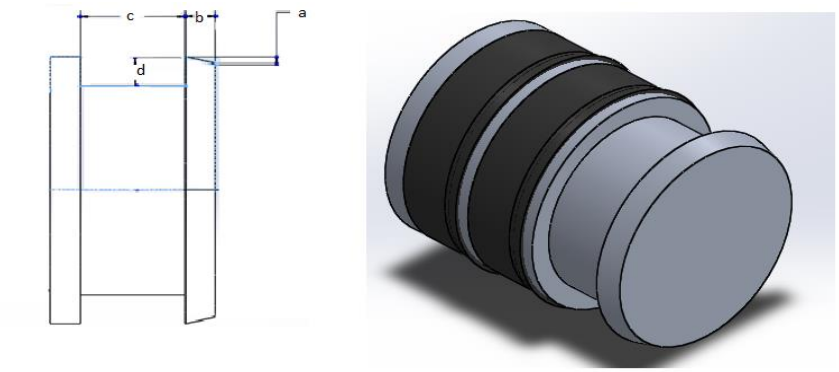

Figure 5. shows (a). The diagram of the crevice region of the piston (b). An isometric view of the angle channel design showing the crevice volume.

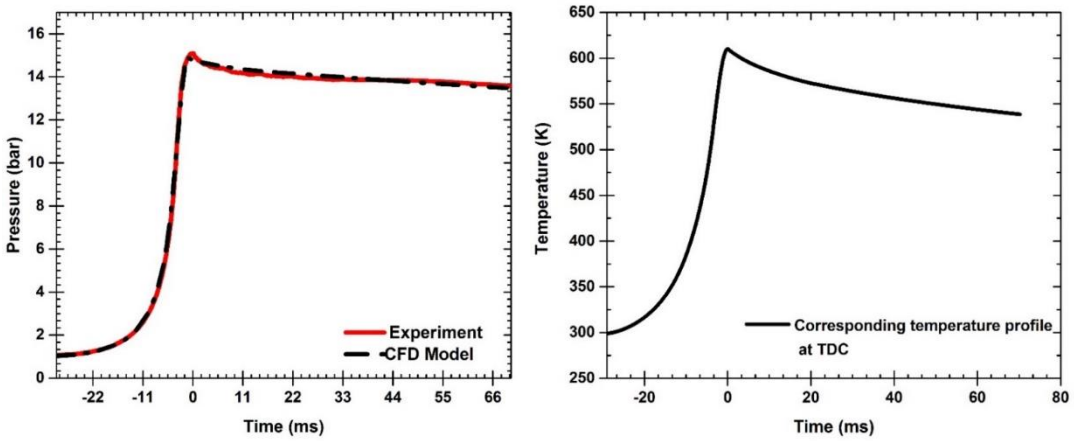

Figure 6. (a) Comparison of Experimental pressure trace with the CFD Model (b) End of compressed gas temperature corresponding to P_C =15 bar, T_C = 615 K.

4. Conclusion

The CFD modelling demonstrated that the use of flat piston generates a roll-up vortex, which could distort the temperature uniformity of the chamber. The results showed that proper machining a crevice on the peripheral surface of the piston could control the vortex build up from the walls of the chamber and maintain the temperature homogeneity of the chamber. The simulation has shown that piston crevice with about 2% of the entire reaction chamber volume was the best for the present RCM. The model result from CFD was machined and tested experimentally. At both compression and post compression period, the model was in agreement with the experimental pressure trace.

References

[1] Westbrook C K, Pitz W J and Herbinet O 2009 A comprehensive detailed chemical kinetic reaction mechanism for combustion of n-alkane hydrocarbons from n-octane to n-hexadecane *Combustion and Flame* **156** 181-99

[2] Curran H J, Gaffuri P and Pitz W 2002 A comprehensive modeling study of iso-octane oxidation *Combustion and flame* **129** 253-80

[3] Dooley S, Curran H J and Simmie J M 2008 Autoignition measurements and a validated kinetic model for the biodiesel surrogate, methyl butanoate *Combustion and Flame* **153** 2-32
[4] Mittal G, Burke S M and Davies V A 2014 Autoignition of ethanol in a rapid compression machine *Combustion and Flame* **161** 1164-71
[5] Mittal G and Sung C-J 2009 Autoignition of methylcyclohexane at elevated pressures *Combustion and Flame* **156** 1852-55
[6] Cowart J S, Keck J C and Heywood J B 1990 Engine knock predictions using a fully detailed and a reduced chemical kinetic mechanism *Proc. Combust. Inst.* **23** 1055-62
[7] Griffiths J F, Jiao Q and Schreiber M 1992 Development of thermokinetic models for autoignition in a CFD Code: Experimental validation and application of the results to rapid compression studies *Symposium (International) on Combustion* **24** 1809-15
[8] Desgroux P, Gasnot L and Sochet L R 1995 Instantaneous temperature measurement in a rapid-compression machine using laser Rayleigh scattering *Applied Physics B Laser and Optics* **61** 69-72
[9] Lee D and Hochgreb S 1998 Rapid compression machines: Heat transfer and suppression of corner vortex *Combustion and Flame* **114** 531-45
[10] Griffiths J F, MacNamara, J P and Mohamed C 2001 Temperature fields during the development of autoignition in a rapid compression machine *Faraday Discussions* **119** 287-303
[11] Mittal G and Sung C J 2006 Aerodynamics inside a rapid compression machine, *Combustion and Flame* **145** 160-80
[12] Würmel J and Simmie J M 2005 CFD studies of a twin-piston rapid compression machine *Combustion and Flame* **141** 417-30
[13] Park P and Keck J C 1990 Rapid compression machine measurements of ignition delays for primary reference fuels *SAE Technical Paper*
[14] Park P 1990 *Rapid compression machine measurements of ignition delays for primary reference fuels* (Cambridge:Massachusetts Institute of Technology)
[15] Mittal G 2006 A Rapid Compression Machine – Design, Characterization, and Autoignition Investigations (Cleveland:Case Western Reserve University)
[16] Mittal G and Sung C-J 2006 Aerodynamics inside a rapid compression machine *Combustion and Flame* **145** 160-80
[17] Brett L, MacNamara J and Musch P 2001 Simulation of methane autoignition in a rapid compression machine with creviced pistons *Combustion and flame* **124** 326-29
[18] Lee D and Hochgreb S 1998 Rapid Compression Machines: Heat Transfer and Suppression of Corner Vortex *Combustion and Flame* **114** 531-45
[19] Griffiths J F, Piazzesi R and Sazhina E M 2012 CFD modelling of cyclohexane auto-ignition in an RCM *Fuel* **96** 192-203
[20] Lemmon E, McLinden M and Friend D 2011 Thermophysical Properties of Fluid Systems in NIST Chemistry WebBook *NIST Standard Reference Database Number 69*, Ed Linstrom P J and Mallard WG (Gaithersburg:National Institute of Standards and Technology)
[21] Goldsborough S S and Potokar C J 2007 The influence of crevice flows and blow-by on the charge motion and temperature profiles within a Rapid Compression Expansion Machine used for chemical kinetic (HCCI) studies *SAE Paper* 01-0169
[22] Mittal G and Chomier M 2013 Interpretation of experimental data from rapid compression machines without creviced pistons *Combustion and Flame*
[23] Issa R I, Gosman A D and Watkins A P 1986 The computation of compressible and incompressible recirculating flows by a non-iterative implicit scheme *Journal of Computational Physics* **62** 66-82
[24] Anderson J D 1995 *Computational fluid dynamics* vol 206 (New York: McGraw-Hill)
[25] Mittal G, Raju M P and Sung C-J 2008 Computational fluid dynamics modeling of hydrogen ignition in a rapid compression machine *Combustion and Flame* **155** 417-28